Enhanced Cellular Uptake of Peptide-Targeted Nanoparticles through Increased Peptide Hydrophilicity and Optimized Ethylene Glycol Peptide-Linker Length

Jared F. Stefanick,[†] Jonathan D. Ashley,[†] and Basar Bilgicer[†,‡,§,*]

[†]Department of Chemical and Biomolecular Engineering, University of Notre Dame, Notre Dame, Indiana 46556, United States, [‡]Department of Chemistry and Biochemistry, University of Notre Dame, Notre Dame, Indiana 46556, United States, and [§]Advanced Diagnostics and Therapeutics, University of Notre Dame, Notre Dame, Indiana 46556, United States

ABSTRACT Ligand-targeted nanoparticles are emerging drug delivery vehicles for cancer therapy. Here, we demonstrate that the cellular uptake of peptide-targeted liposomes and micelles can be significantly enhanced by increasing the hydrophilicity of the targeting peptide sequence while simultaneously optimizing the EG peptide-linker length. Two distinct disease models were analyzed, as the nanoparticles were functionalized with either VLA-4 or HER2 antagonistic peptides to target multiple myeloma or breast cancer cells, respectively. Our results demonstrated that including a short oligolysine chain adjacent to the targeting peptide sequence effectively increased cellular uptake of targeted nanoparticles up to ~80-fold using an EG6 peptide-linker in liposomes and ~27-fold using an EG18 peptide-linker in micelles for the VLA-4/multiple myeloma system. Similar trends were also observed in the HER2/breast cancer system with the EG18 peptide-linker resulting in optimal uptake for both types of nanoparticles. Cellular uptake efficiency of these formulations was also confirmed under fluidic conditions mimicking physiological systems. Taken together, these results demonstrated the significance of using the right design elements to improve the cellular uptake of nanoparticles.

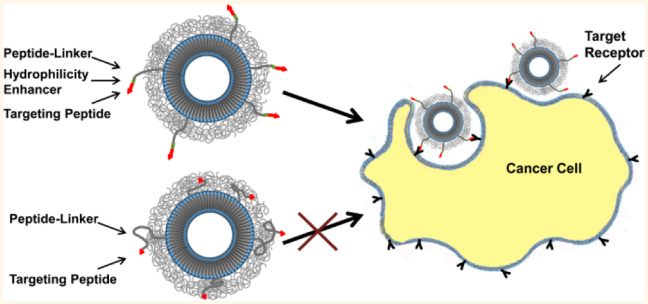

KEYWORDS: VLA-4 · HER2 · peptide-targeted nanoparticles · peptide-linker · cellular uptake · liposome · micelle

Polyethylene glycol (PEG)-coated nanoparticles are widely used drug delivery vehicles for the selective delivery of therapeutic agents, notably for cancer therapy.[1,2] The PEGylation of both liposomal and micellar drug formulations results in nanoparticles with increased stability, bioavailability, and tumor accumulation due to the enhanced permeability and retention effect, which is known as passive targeting.[3−9] In an effort to improve tumor targeting and cellular uptake, nanoparticles can also be functionalized with active targeting molecules such as antibodies, antibody fragments, small molecules, and peptides.[10−13] To date, active targeting approaches, however, have not consistently shown successful outcomes.[14−16] This discrepancy has in part been attributed to the differences in the type of disease models and target receptors. There is, however, also a strong prevalence such that differences in nanoparticle design including the synthetic methods used to prepare the nanoparticles, the linkers used to conjugate the targeting ligands, the type of targeting ligand, and the length and density of liposomal PEG coating significantly contribute to the apparent inconsistent outcomes.

PEG2000 (a mean of ~45 repeating units of ethylene glycol: EG45) is the polymer of choice for coating nanoparticles to enhance *in vivo* circulation by inhibiting immune system detection.[4,17] In order to prepare ligand-targeted nanoparticles, targeting ligands have been traditionally grafted onto the distal end of PEG2000 or longer linkers

* Address correspondence to bbilgicer@nd.edu.

Received for review July 3, 2013 and accepted August 29, 2013.

Published online August 29, 2013
10.1021/nn4033954

such as PEG3350 and PEG5000 to effectively present the ligands above the PEG coating.[9,18−20] However, long PEG polymers do not preserve a linear conformation in the aqueous phase; instead, they fold within themselves to form mushroom-like, globular structures.[21−23] This unique morphology significantly lowers the percent of accessible ligand by burying it within the PEG coating and sterically hindering the association of the ligand-targeted nanoparticles with their target receptor. Successful demonstrations of ligand-targeted nanoparticles with such longer PEG chains have been largely observed with receptor−ligand pairs that exhibit high binding affinity ($K_d \approx$ low nM), such as the folic acid−folate receptor and antibody−antigen interactions.[2,15] To the contrary, recent studies have demonstrated that for low to moderate affinity ligands shorter EG ligand-linkers can yield more favorable results, highlighting the significance of ligand linker length and ligand−receptor physiochemical properties.[24] Short EG linkers adopt a more linear morphology in the aqueous phase when compared to longer PEG linkers, thereby demonstrating reduced entropic penalties upon binding and resulting in improved ligand activity, which drives increased cellular binding and subsequent uptake of targeted liposomes.

Cyclic peptides are gaining popularity as targeting ligands because of the advantages they provide including ease of preparation, lower cost, lower antigenicity, decreased opsonization, and increased resistance to enzymatic degradation *in vivo*.[25−27] Peptides can be conjugated to lipids to generate amphiphilic molecules, which can be readily incorporated into liposomes or micellar nanoparticles during their formation, allowing for precise control over the stoichiometry of targeting ligands with high reproducibility.[24,28] However, biophysical and chemical properties of peptides may affect their efficacy as targeting agents in a nanoparticle platform.[29−31] For example, hydrophobic peptide sequences can promote nanoparticle aggregation or become buried in the lipid segment of the liposome or micelle, reducing ligand accessibility and increasing nanoparticle size. Limited chemical stability with respect to either the synthetic techniques for creating nanoparticles or physiological pH and temperature can also compromise peptide activity.[32−34] These combined factors may limit the therapeutic potential of peptide-targeted nanoparticles.

In this study, we demonstrated that the targeting efficiency of peptide-targeted nanoparticles can be dramatically enhanced by (i) increasing the hydrophilicity of the targeting peptide sequence and (ii) systematic optimization of the EG peptide-linker length. To validate our strategy, first we evaluated the effect of peptide hydrophilicity and EG linker-length on the cellular uptake of very late antigen-4 (VLA-4; also known as $\alpha_4\beta_1$ integrin) targeted liposomes and micelles. In our approach, we used a short cyclic peptide antagonist of VLA-4 as the targeting ligand and identified the optimal design elements for maximum cellular uptake by VLA-4-overexpressing multiple myeloma cells. We then validated our findings by applying and evaluating the optimized design elements in a human epidermal growth factor receptor 2 (HER2)-overexpressing breast cancer model. In both disease models, we consistently demonstrated that cellular uptake of nanoparticles is significantly enhanced by increasing the peptide hydrophilicity through the addition of a short oligolysine chain (K_N, where K refers to the lysines and *N* is number of repeat units) adjacent to the peptide-targeting ligand and optimizing the EG peptide-linker length to compromise between peptide presentation beyond the PEG cloud and compensation of entropic losses from long linkers. These results established the significance of using the right design elements in the efficient targeting of tumors.

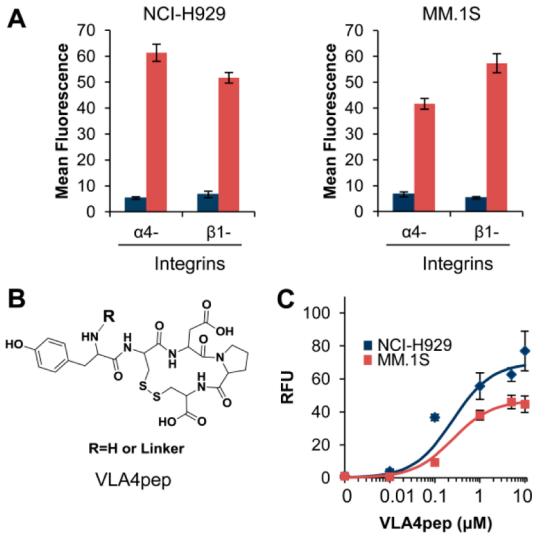

Figure 1. VLA-4 expression in multiple myeloma cancer cells and identification of a VLA-4-antagonist peptide. (A) NCI-H929 and MM.1S myeloma cells express VLA-4 subunits α_4- and β_1-integrins as determined by flow cytometry. Red columns are primary antibodies, and blue columns are isotype controls. (B) Structure of VLA-4-antagonist peptide (VLA4pep). (C) Cellular binding using fluorescein-labeled VLA4pep was detected by flow cytometry.

RESULTS AND DISCUSSION

Validation of the Selective Binding of a VLA-4-Antagonist Peptide to VLA-4-Overexpressing Multiple Myeloma Cells. We validated the $\alpha_4\beta_1$ integrin expression levels in NCI-H929 and MM.1S multiple myeloma cell lines *via* flow cytometry by using fluorescently labeled, integrin-specific antibodies (Figure 1A). Due to the critical role of VLA-4 in cancers, several antagonistic peptides have been identified.[35−37] The cyclic peptide sequence YCDPC (VLA4pep; Figure 1B) has been shown to bind to VLA-4-expressing myeloma cells with specificity and was therefore selected for this study.[28] We validated

selective binding of VLA4pep to NCI-H929 and MM.1S cells by labeling VLA4pep with fluorescein and analyzing its binding to cells by flow cytometry (Figure 1C). Control experiments performed with a fluorescein-labeled scrambled peptide showed only minimal background binding, which was subtracted from each data point. VLA4pep bound to both myeloma cell lines with an apparent K_d of 250 nM.

Design and Preparation of Peptide-Targeted Liposomes and Micelles. The physiochemical properties of peptide-based targeting ligands and the length of the EG peptide-linker are important parameters for actively targeted nanoparticles.[24,31] To assess the effect of peptide hydrophilicity and EG peptide-linker length on the cellular uptake of peptide-targeted nanoparticles, we synthesized several peptide(K_N)-EG_{linker}-lipid conjugates (Figure 2A). In our design, the conjugates consist of (i) a receptor-specific peptide (*i.e.*, VLA4pep), (ii) an EG2 spacer, (iii) a short oligolysine chain (K_N, where K refers to the lysines and *N* is number of repeat units) to increase hydrophilicity, (iv) an EG peptide-linker, and (v) two hydrophobic fatty acid chains to enable insertion into the lipid bilayer of the liposomes or associate with the lipid core of micelles. An EG2 spacer minimizes interactions between the peptide and the oligolysine chain (K_N), and an EG peptide-linker, which varies from EG6 to EG72, aids in presenting the targeting peptide beyond the PEG cloud on the nanoparticles to enable binding to the target receptor. The two fatty acid chains were coupled to the EG linker *via* first coupling L-lysine to the N-terminus of the EG linker and then coupling the fatty acids to the α- and ε-amines of the L-lysine residue to generate the hydrophobic tail of the peptide-(K_N)-EG_{linker}-lipid conjugate. Palmitic acid was selected in lieu of a conventional carboxylic acid-terminated phospholipid, such as DPPE-GA or DSPE-GA, due to its greater chemical stability, as it lacks the phosphoester bond and increased solubility in typical solid phase reagents such as DCM and DMF. The synthesis of the peptide(K_N)-EG_{linker}-lipid conjugates was carried out entirely on a solid support platform using standard Fmoc chemistry protocols. Completed products were then

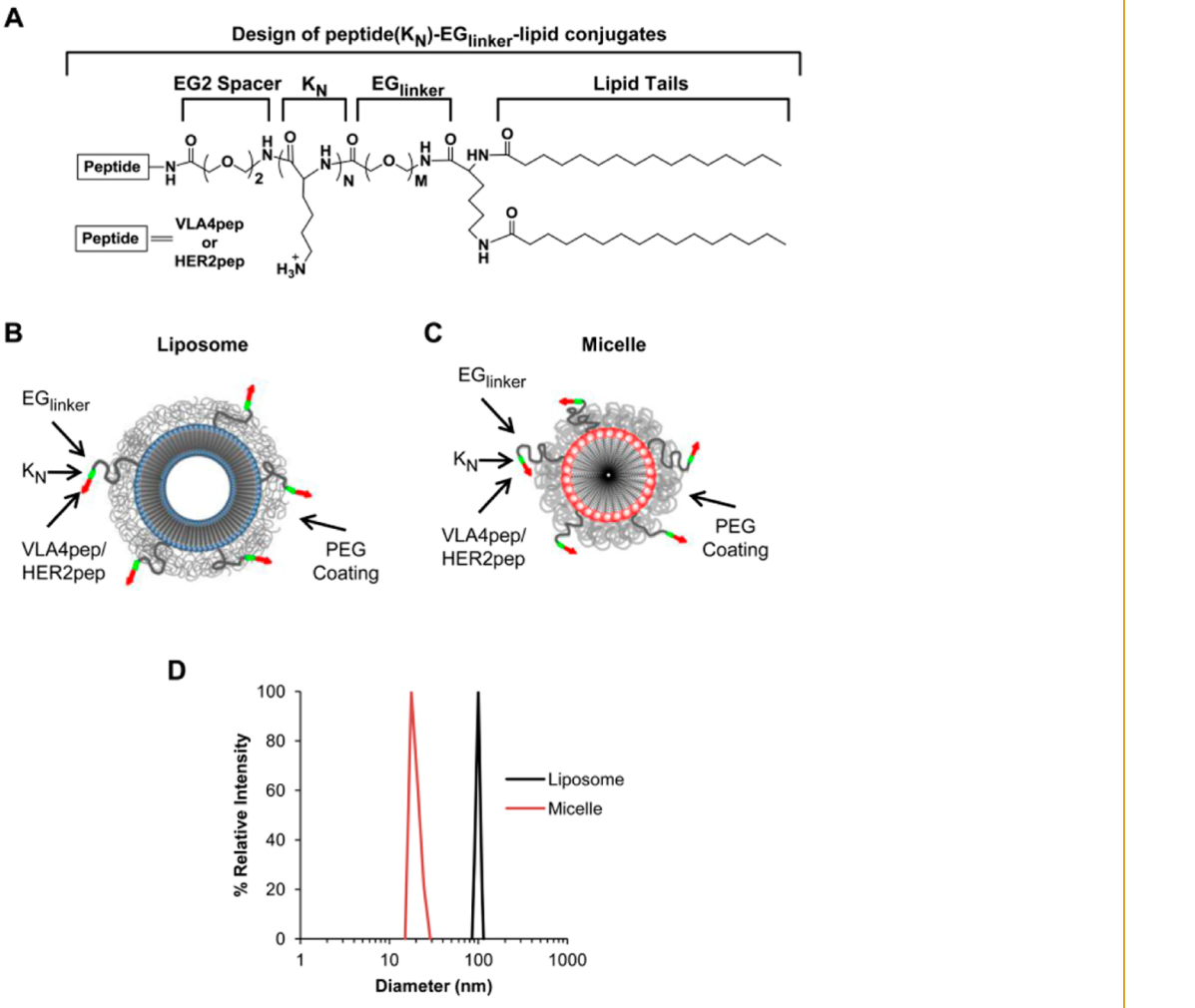

Figure 2. Design and characterization of peptide-conjugated nanoparticles. (A) Structure of peptide(K_N)-EG_{linker}-lipid conjugates with variable oligolysine (K_N) content and EG peptide-linker lengths including EG6, EG12, EG18, EG24, EG30, EG36, EG45, and EG72. (B) Schematic of the peptide-targeted liposomes. (C) Schematic of peptide-targeted micelles. (D) Dynamic light scattering analysis of nanoparticles.

cleaved from the resin and purified *via* RP-HPLC. Peptide cyclization through disulfide bond formation was performed in DMF with DIEA at room temperature while stirring overnight. Full synthetic scheme, mass spectrometry data, and product yields of the synthesized peptide(K_N)-EG_{linker}-lipid conjugates are provided (see Supporting Information, Figure S1 and Table ST1).

Liposomes (Figure 2B) were prepared using purified peptide(K_N)-EG_{linker}-lipid conjugates, PEG2000-DSPE, HSPC, and cholesterol, while micelles (Figure 2, C) were prepared with peptide(K_N)-EG_{linker}-lipid conjugates and PEG2000-DSPE to yield nanoparticles around 100 nm and 15−20 nm, respectively, as determined by dynamic light scattering (DLS) (Figure 2D). The components were mixed at specific stoichiometries to achieve precise control over the number of functional ligands on each particle, maintaining reproducibility in nanoparticle production.[24,28] The liposomes were sized *via* extrusion through a polycarbonate membrane, while micelles were formed by solvent evaporation and sonication, at lipid concentrations above the critical micelle concentration of 5−10 μM to create relatively monodisperse particles with ~90 lipid molecules per micelle.[38,39] Fluorescein PE was incorporated into the nanoparticles for cellular uptake experiments at 0.2% or 1% phospholipid concentration for liposomal flow cytometry or microscopy experiments, respectively, and 1 or 5 lipids per micelle for micellar flow cytometry or microscopy experiments, respectively. Regardless of the nanoparticle formulation, including the addition of fluorescent imaging agents or targeting moieties, the mean diameter of the particles remained constant (see Supporting Information, Table ST2 for particle size and zeta potential analysis of select nanoparticle formulations).

Effect of EG Peptide-Linker Length, Oligolysine Content (K_N), and Peptide Valency on the Cellular Uptake of VLA-4-Targeted Liposomes. The length of the EG peptide-linker connecting the targeting peptide to the lipid anchor is an important parameter for consideration in the design of peptide-targeted liposomes. Therefore, to evaluate this, we examined the effect of the EG peptide-linker length on cellular uptake of liposomes by using VLA4-pep with no lysines (VLA4pep(K_0)) tethered to a variety of linkers including EG6, EG12, EG18, EG24, EG30, EG36, EG45, and EG72 (Figure 3A). Targeted liposomes were formulated as 93:10:5:2 HSPC:CHOL:PEG2000:VLA4pep(K_0) with a nontargeted control of 95:10:5 HSPC:CHOL:PEG2000. Our results showed that, regardless of EG linker length, there was only minimal uptake despite the high density of VLA4pep(K_0) on the surface of the liposomes. Given that the research standard for preparing ligand-targeted liposomes has traditionally involved attaching the targeting ligand onto the distal end of functionalized PEG polymers that are at least

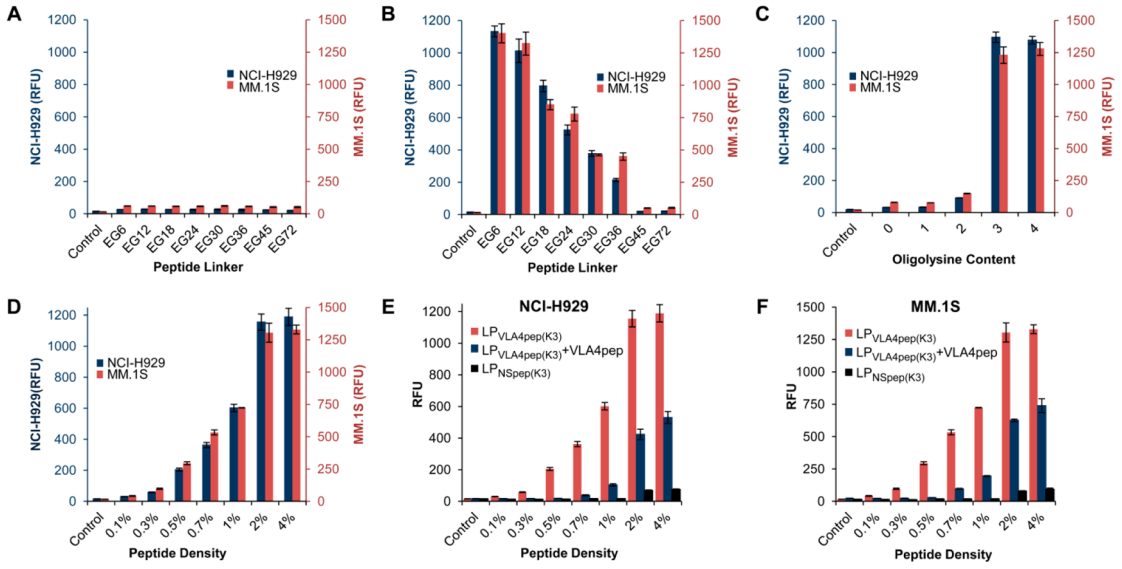

Figure 3. Effect of EG peptide-linker length, oligolysine (K_N) content, and peptide valency on the cellular uptake of VLA-4-targeted liposomes. (A) Effect of EG peptide-linker length on the cellular uptake of liposomes targeted with VLA4pep(K_0) evaluated with NCI-H929 (blue columns) and MM.1S (red columns) cells by flow cytometry. The EG linker lengths investigated include EG6, EG12, EG18, EG24, EG30, EG36, EG45, and EG72. (B) Effect of EG peptide-linker length on the uptake of liposomes targeted with VLA4pep(K_3). Cellular uptake by NCI-H929 (blue columns) and MM.1S (red columns) cells was determined by flow cytometry. (C) Effect of oligolysine chain length (K_N) evaluated using liposomes targeted with VLA4pep(K_N) using an EG6 peptide-linker. Cellular uptake by NCI-H929 (blue columns) and MM.1S (red columns) cells was evaluated by flow cytometry. The K_N chain length varied in the range $N = 0-4$. (D) Effect of peptide valency of the cellular uptake of liposomes targeted with VLA4pep(K_3) ($LP_{VLA4pep(K3)}$) with an EG6 peptide-linker. Peptide density was varied between 0 and 4% of the total lipid, and cellular uptake was evaluated for NCI-H929 (blue columns) and MM.1S (red columns). (E) Competition experiments performed with excess free VLA4pep to determine specificity of uptake for NCI-H929 cells. (F) Competition experiments performed with excess free VLA4pep to determine specificity of uptake for MM.1S cells. Nonspecific peptide (NSpep) was also incorporated into liposomes ($LP_{NSpep(K3)}$) as a control (black column). All experiments were done in triplicates, and data represent means (±SD).

45 EG units in length (PEG2000),[9] this observation was unexpected. We attributed the lack of uptake to limited peptide accessibility, as the shorter EG linkers may not effectively expose the peptide beyond the PEG2000 coating and the longer EG linkers may bury the peptide in the PEG2000 coating due to the globular, mushroom-like morphology.

In order to increase cellular uptake, we hypothesized that the binding activity of VLA-4-targeted liposomes can be enhanced by increasing the hydrophilicity of the peptide targeting sequence through the incorporation of lysine (K_N) residues adjacent to the peptide (Figure 2A). Therefore, we next evaluated the effect of the chemical properties of the targeting peptide, specifically its hydrophilicity, in coordination with the EG peptide-linker length to increase peptide availability to bind to its target receptor. For this, we synthesized VLA4pep with three lysine residues (VLA4pep(K_3)) and examined the effect of EG linker length on cellular uptake by tethering VLA4pep(K_3) to EG linkers ranging from EG6 to EG72 (Figure 3B). Targeted liposomes were formulated as 93:10:5:2 HSPC:CHOL:PEG2000:VLA4pep-(K_3). Our results demonstrated a dramatic increase in cellular uptake of targeted liposomes, with maximum enhancements of ~75- and ~85-fold for NCI-H929 and MM.1S myeloma cell lines, respectively, using the EG6 linker. We predict that the addition of the oligolysine chain (K_3) simultaneously increased hydrophilicity and improved exposure beyond the PEG coating, increasing the display of the peptide in the aqueous portion of the liposome exterior and enhancing the availability of VLA4pep to bind to its target receptor. The uptake enhancement declined with increasing EG peptide-linker length, completely diminishing with EG45 and EG72 linkers.

Given that longer linkers, such as EG45 (PEG2000), have traditionally been used for ligand-targeted nanoparticles, it is interesting, but not altogether unexpected, that shorter peptide-linkers, such as EG6, yielded greater enhancements in cellular uptake. Longer PEG linkers provide a steric hindrance to ligand binding due to the mushroom-like globular structure and provide less thermodynamically favorable interactions. Conversely, shorter linkers can restrict the translational and conformational freedom of the peptide, thereby reducing the overall entropic loss when the liposome binds to the cell. Furthermore, a shorter linker can adopt a more linear conformation, unlike a longer linker. Although PEG2000 consists of a mean of 45 EG repeat units, which is ~16 nm in length when linear, hydration studies have shown that PEG2000 actually extends only ~3−5 nm from the surface of the liposome due to the mushroom-like structure.[22,23] The EG6 peptide-linker extends a net distance of ~5.5 nm from the lipid head to VLA4pep, which is sufficiently long enough to span through the PEG2000 cloud when linear. This provides a more favorable interaction, which results in improved cellular binding and subsequent uptake.

Next, to assess the optimal oligolysine chain length, we synthesized VLA4pep(K_N) with an EG6 peptide-linker, varied *N* from 0 to 4, and evaluated cellular uptake (Figure 3C). Targeted liposomes were formulated as 93:10:5:2 HSPC:CHOL:PEG2000:VLA4pep(K_N). Our results showed minimal cellular uptake with the incorporation of zero to two lysine residues, but the inclusion of three lysines resulted in a significant enhancement and reached a plateau for cellular uptake.

We then examined the effect of peptide valency on cellular uptake. We prepared targeted liposomes containing VLA4pep(K_3) with an EG6 linker ((95 − *x*):10:5:*x* HSPC:CHOL:PEG2000:VLA4pep(K_3), where *x* represents the peptide valency) to find the optimal conditions for maximal uptake (Figure 3D). For both myeloma cell lines, the uptake reached a maximum and a plateau at 2% peptide density, likely due to the saturation of cellular uptake mechanisms. Competition experiments performed with excess free VLA4pep demonstrated efficient inhibition of uptake, establishing the specificity of receptor−ligand interactions and the involvement of VLA-4 receptor in the uptake of targeted liposomes (Figure 3E and F). In an additional control experiment, only negligible uptake was observed with liposomes that incorporated a nonspecific peptide (NS) with three lysines and EG6 linker (NSpep(K_3)), further establishing the selectivity and specificity of the uptake observed for VLA-4-targeted liposomes. Pharmacological inhibition of endocytosis was also applied to investigate the entry mechanism of the liposomes into cells. The cellular uptake of targeted liposomes (93:10:5:2 HSPC:CHOL:PEG2000:VLA4pep(K_3)) was significantly inhibited by chlorpromazine and chloroquine, indicating that the liposomes entered the cells *via* clathrin-mediated endocytosis (see Supporting Information, Figure S2). Minor inhibition was also observed using EIPA, demonstrating that macropinocytosis was also involved in cellular uptake.

Effect of EG Peptide-Linker Length, Oligolysine Content (K_N), and Peptide Valency on the Cellular Uptake of VLA-4-Targeted Micelles. In order to further validate our targeting strategy and determine if the results obtained with the liposomes can be applied broadly to other drug delivery systems, we evaluated our approach with micellar nanoparticles. Although micelles are another type of lipid-based drug delivery vehicle, their smaller size (~15−20 nm diameter), decreased number of lipids per particle (~90 lipids per micelle compared to ~80 000 lipids per 100 nm diameter liposome), and absence of a lipid bilayer provide noticeable differences compared to liposomes.[22,38] To evaluate the effect of the EG peptide-linker length on the cellular uptake of VLA-4-targeted micelles, we formulated micelles that incorporated VLA4pep with no lysines

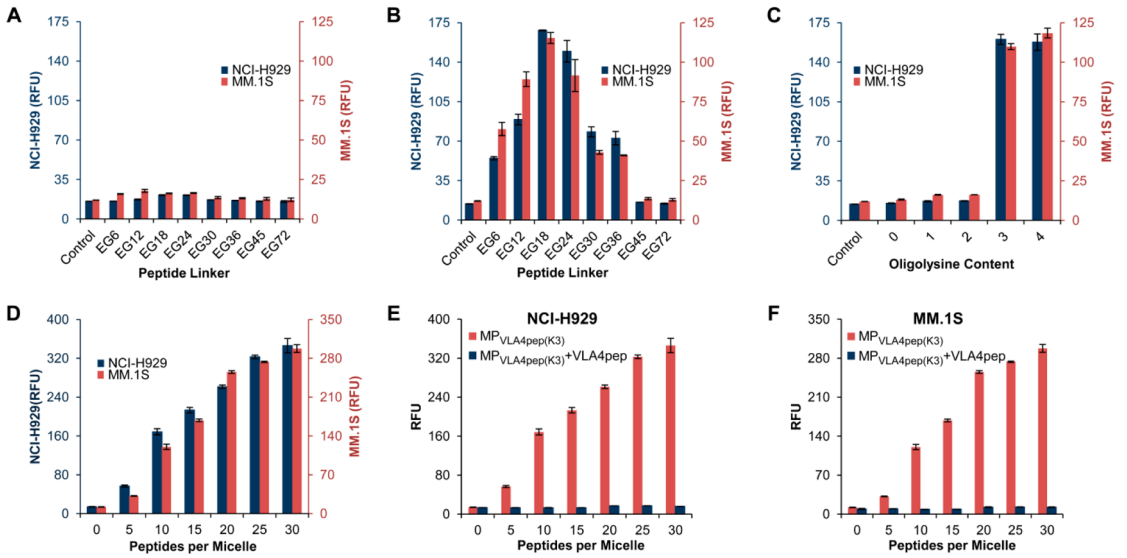

Figure 4. Effect of EG peptide-linker length, oligolysine (K_N) content, and peptide density on the cellular uptake of VLA-4-targeted micelles. (A) Effect of EG peptide-linker length on the cellular uptake of micelles targeted with VLA4pep(K_0) evaluated using NCI-H929 (blue columns) and MM.1S (red columns) cells by flow cytometry. The EG peptide-linker lengths investigated include EG6, EG12, EG18, EG24, EG30, EG36, EG45, and EG72. (B) Effect of EG peptide-linker length on the uptake of micelles targeted with VLA4pep(K_3). Cellular uptake by NCI-H929 (blue columns) and MM.1S (red columns) cells was determined by flow cytometry. (C) Effect of oligolysine chain length (K_N) evaluated using micelles targeted by VLA4pep(K_N) with EG18 peptide-linker. Cellular uptake by NCI-H929 (blue columns) and MM.1S (red columns) cells was evaluated by flow cytometry. The K_N content varied in the range $N = 0-4$. (D) The effect of peptide valency of the cellular uptake of micelles targeted with VLA4pep(K_3) ($MP_{VLA4pep(K3)}$) using an EG18 peptide linker. Peptide density was varied from 0 to 30 peptides per micelle, and cellular uptake was evaluated for NCI-H929 (blue columns) and MM.1S (red columns). (E) Competition experiments performed with excess free VLA4pep to determine specificity of uptake for NCI-H929 cells. (F) Competition experiments performed with excess free VLA4pep to determine specificity of uptake for MM.1S cells. All experiments were done in triplicates, and data represent means (±SD).

(VLA4pep(K_0)) and variable EG linker lengths of EG6, EG12, EG18, EG24, EG30, EG36, EG45, and EG72 (Figure 4A). Targeted micelles were formulated as 80:10 PEG2000:VLA4pep(K_0). Similar to the liposomes, we did not observe improved cellular uptake through the EG peptide-linker length modification alone. However, when we increased the hydrophilicity of VLA4-pep through the addition of three lysines (VLA4pep(K_3)) and evaluated the cellular uptake of micelles targeted with VLA4pep(K_3) (80:10 PEG2000:VLA4pep(K_3)), we observed a bell-shaped distribution with respect to EG peptide-linker length, with maximum uptake using an EG18 linker (Figure 4B). These results are similar to the ones observed with liposomes, as increasing the hydrophilicity of the peptide ligand significantly increased cellular uptake. In addition, traditional formulations using an EG45 or EG72 peptide linker showed negligible uptake for both myeloma cells lines. One notable difference was the optimal EG linker length for the liposomes (EG6, extension distance ~5.5 nm) *versus* micelles (EG18, extension distance ~10.1 nm), which can be due to the PEG surface morphology and curvature of the micelles. In the micellar structure, PEG2000 adopts a more brush-like structure as opposed to the mushroom shape in the liposomes,[40] extending the PEG cloud further away from the lipid layer. Furthermore, the smaller size of the micelles significantly reduces the surface area of interaction between the micelle and the cell surface, as these micelles have only ~15−20 nm diameter (~3000 nm^2 total surface area), compared to a 100 nm liposome (~125 000 nm^2 total surface area). Thus, a longer linker is necessary to sufficiently expose the peptide to initiate the multivalent binding interactions required for cellular uptake.

In order to determine if three lysine residues provided optimal cellular uptake for this system as well, we assessed the optimal oligolysine chain length on the cellular uptake of micelles by synthesizing VLA4pep(K_N) with an EG18 peptide-linker and varying *N* from 0 to 4 (Figure 4C). Targeted micelles were formulated as 80:10 PEG2000:VLA4pep(K_N). Our results showed minimal uptake with the incorporation of zero to two lysine residues, but a significant enhancement was observed with the inclusion of three lysines. This is in agreement with results demonstrated previously with the liposomes, suggesting that the oligolysine content of three units sufficiently increased the peptide hydrophilicity in order to more effectively present the peptide above the PEG2000 coating for binding and uptake of nanoparticles.

To examine the relationship between peptide valency and cellular uptake, we prepared targeted micelles containing VLA4pep(K_3) with EG18 linker, where the valency was varied from 0 to 30 peptides per micelle (Figure 4D). The uptake efficacy reached

a maximum and approached a plateau at higher densities with ~27-fold enhancement for both cell lines at 30 peptides per micelle. To verify the specificity of the observed interaction, competition experiments in the presence of free VLA4pep were performed (Figure 4E and F), which showed significant inhibition, demonstrating specificity and receptor involvement in uptake. Pharmacological inhibition of endocytosis was also applied to investigate the entry mechanism of the micelles. The cellular uptake of targeted micelles (80:10 PEG2000:VLA4pep(K_3)) was significantly inhibited by chlorpromazine and chloroquine with minor inhibition by EIPA, indicating that the micelles predominantly entered the cells *via* clathrin-mediated endocytosis (see Supporting Information, Figure S3).

Validation of Cellular Uptake Results with Confocal Microscopy. While flow cytometry is a powerful tool to quantify association of nanoparticles with cells, it does not distinguish between cellular binding and cellular internalization. To confirm cellular uptake and internalization of the nanoparticles by the multiple myeloma cells, we performed confocal microscopy experiments with fluorescein-labeled liposomes (93:10:5:2 HSPC:CHOL:PEG2000:VLA4pep(K_3)) and micelles (80:10 PEG2000:VLA4pep(K_3)). Nontargeted nanoparticles and cell-only controls were also included. Intracellular acidic vesicles (endosomes/lysosomes) were labeled with LysoTracker Red, and the co-localization of the nanoparticles in intracellular vesicles was examined. In both NCI-H929 and MM.1S cell lines, we observed significant internalization into lysosomes with targeted formulations, with no internalization evident with nontargeted nanoparticles (Figure 5A and B). Additional confocal microscopy images at higher magnification are also provided (see Supporting Information, Figure S4).

Effect of EG Peptide-Linker Length and Oligolysine Content (K_N) on the Cellular Uptake of HER2-Targeted Liposomes and Micelles. To confirm that the conclusions derived from the experiments presented with VLA-4-targeting liposomes and micelles can be applied broadly to other peptide-targeted delivery systems, we have undertaken a similar analysis with HER2-overexpressing breast cancer cells. HER2 is overexpressed in ~25% of breast cancer cases, and several cell lines have been identified to overexpress HER2 including SK-BR-3 and BT-474 cells.[41,42] First, we validated HER2 receptor expression in SK-BR-3 cells (see Supporting Information, Figure S5A). Several antagonistic peptides of HER2 have been identified.[43−45] The cyclic peptide sequence, YCDGFYACYMDV (HER2pep; Figure 6A), has been reported to bind to an extracellular HER2 domain with submicromolar affinity (K_d = 150 nM).[46] We determined selective binding of this peptide to SK-BR-3 cells by flow cytometry using a fluorescein-labeled version of the peptide (see Supporting Information, Figure S5B).

We then prepared HER2-targeted liposomal and micellar nanoparticles with variable oligolysine content (K_N; N = 0 or 3) and EG peptide-linker length (EG6 to EG72) to analyze cellular uptake in SK-BR-3 cells by flow cytometry. Our results obtained with the HER2-targeting system demonstrated consistent results with the VLA-4 system. When HER2pep with no lysines (HER2pep(K_0)) was incorporated into the targeted liposomes (93:10:5:2 HSPC:CHOL:PEG2000:HER2pep(K_0)), we observed no enhancement in cellular uptake regardless of EG peptide-linker length (Figure 6B). However, incorporation of HER2pep with a short oligolysine chain (HER2pep(K_3)) in the targeted formulation (93:10:5:2 HSPC:CHOL:PEG2000:HER2pep(K_3)) resulted in a significant enhancement in cellular uptake, reaching a maximum with an EG18 peptide-linker. Similarly, micelles targeted with HER2pep(K_0) (75:15 PEG2000:HER2pep(K_0)) displayed minimal uptake across the various EG linker lengths examined, while micelles targeted with HER2pep(K_3) (75:15 PEG2000:HER2pep(K_3)) were efficiently taken up by the cells, with maximum uptake observed using an EG18 peptide-linker as well (Figure 6C). These results demonstrated that the cellular uptake of both HER2-targeted liposomes and micelles can be significantly enhanced by increasing the peptide hydrophilicity and optimizing the EG peptide-linker length. One minor difference between the VLA-4- and HER2-targeted liposomes was that while an EG6 peptide-linker was optimal for the VLA-4 system, an EG18 linker was optimal for the HER2 system. This is likely due to the distinct chemical properties for each targeting peptide. HER2pep is a 12-residue peptide compared to the five-residue VLA4pep and is more hydrophobic, with several aromatic residues. Therefore, a longer linker may be required to further increase its aqueous solubility when compared to the VLA4pep. In addition, the particular receptor−ligand interactions and location of the binding pocket could also play a role. The EG18 linker is possibly the optimum distance necessary to allow HER2pep to adopt a proper conformation to bind to the binding pocket on the target receptor and permit multivalent interactions.

To determine the optimal oligolysine chain length necessary for the most efficient cellular uptake, we synthesized HER2pep(K_N) with an EG18 peptide-linker, varied N from 0 to 4, and evaluated cellular uptake for both micelles and liposomes (Figure 6D). Our results showed minimal cellular uptake with zero to two lysines, but a significant enhancement was observed with the inclusion of three lysines. Confirmation of nanoparticle uptake was also demonstrated through co-localization studies performed with the lysosomal marker LysoTracker Red and fluorescein-labeled nanoparticles using confocal microscopy. Both liposomes and micelles targeted with HER2pep(K_3) and EG18 linker showed significant internalization into lysosomes (Figure 6E). Additional confocal microscopy images at higher magnification are also provided (see Supporting Information, Figure S6). Collectively, these results were consistent with the VLA-4 targeting

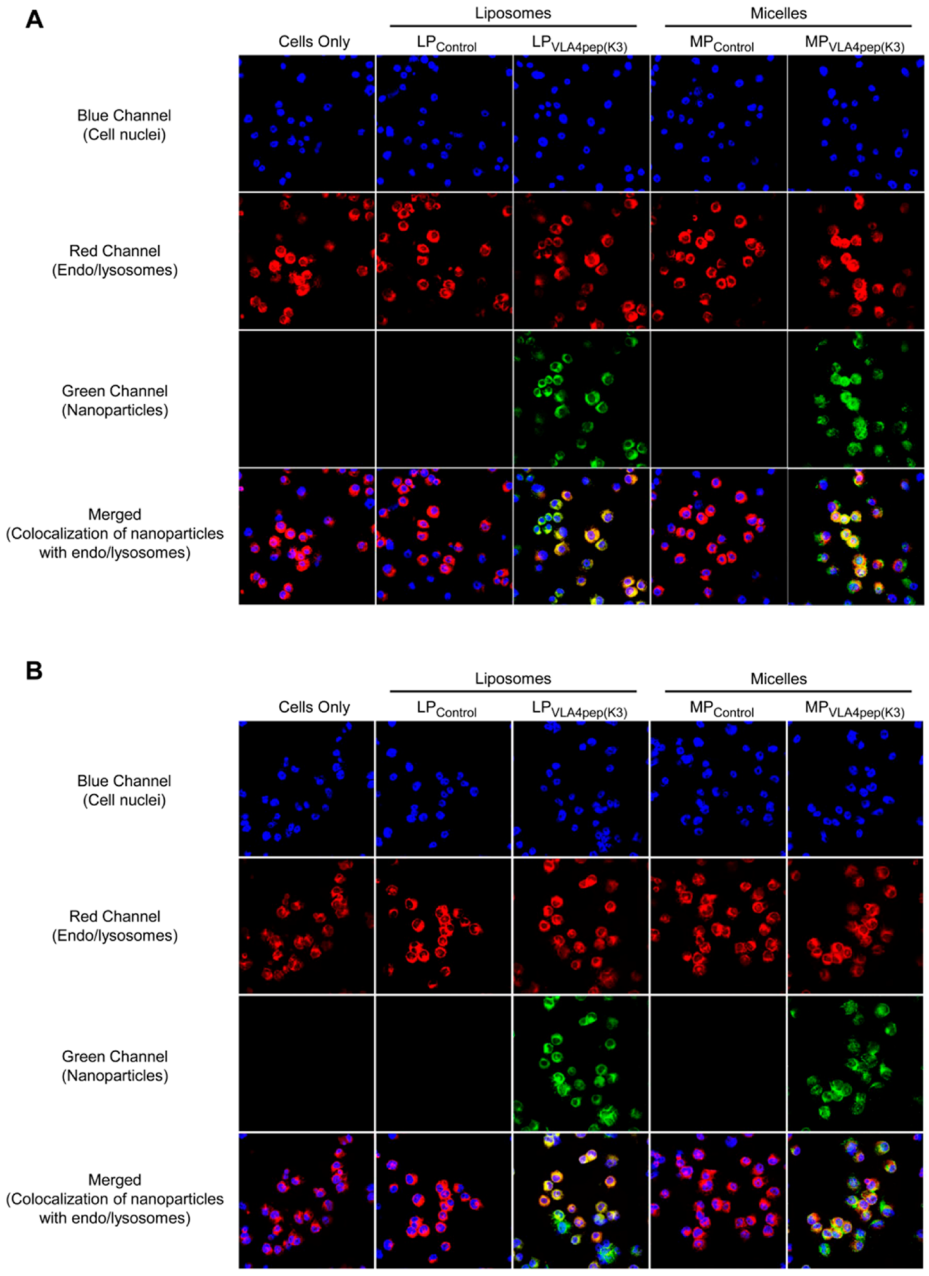

Figure 5. Determination of cellular uptake *via* confocal microscopy. Fluorescein-labeled nanoparticles were incubated with NCI-H929 (A) or MM.1S (B) cells for 3 h at 37 °C. The cells were counterstained with LysoTracker Red and Hoechst dyes. Merged images reveal co-localization. Internalization of nanoparticles was determined with a Nikon A1R confocal microscope using a 40× oil lens. Image acquisition was performed by Nikon Elements Ar software.

system, validating that the conclusions drawn can be applied broadly to other peptide-targeted systems, although exact properties, such as the optimal EG linker length, may differ slightly.

Effect of EG Peptide-Linker Length and Oligolysine Content (K_N) on the Cellular Uptake of Nanoparticles under Fluidic Conditions. To further validate our experimental findings under physiologically relevant conditions, we examined the uptake efficiency of our peptide-targeted nanoparticle formulations under fluidic conditions to mimic those found in physiological systems. Because our study included two cancer cell types with distinct *in vitro* culture conditions (multiple myeloma cells grow in suspension, while breast cancer cells are adherent), we employed two model flow channel systems for use in our experiments (see Supporting Information, Figure S7). For the multiple myeloma system, a peristaltic pump connected to a reservoir was used to load the myeloma cells (NCI-H929 or MM.1S) and nanoparticles into the circulating system. After loading, the reservoir inlet and outlets were connected to create a closed circulating system. This design minimized any cellular uptake of nanoparticles that may have occurred in the reservoir under more static conditions. For the breast

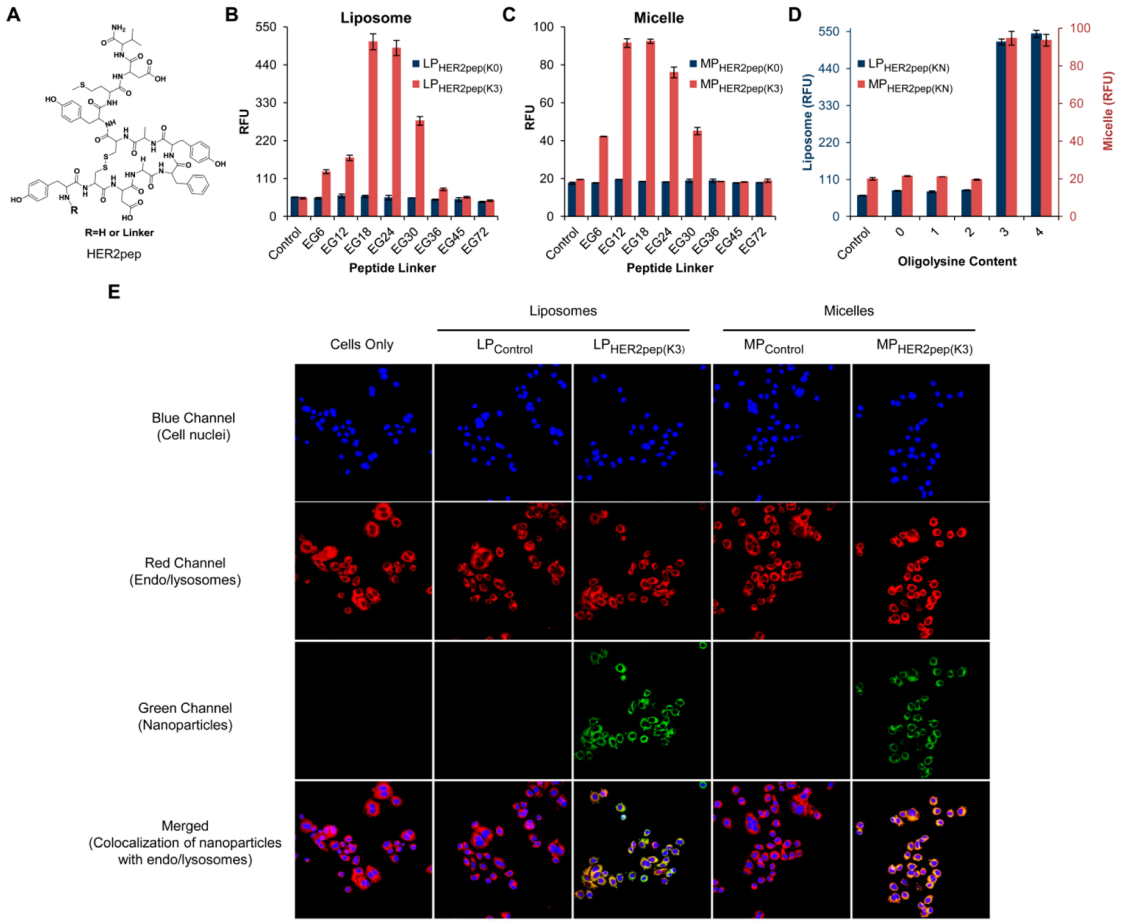

Figure 6. Effect of EG peptide-linker length and oligolysine (K_N) content on the cellular uptake of HER2-targeted liposomes and micelles. (A) Structure of HER2-antagonist peptide (HER2pep). (B) Effect of EG peptide-linker length on the uptake of liposomes targeted with HER2pep(K_0) ($LP_{HER2pep(K0)}$; blue columns) and HER2pep(K_3) ($LP_{HER2pep(K3)}$; red columns) by SK-BR-3 cells. (C) Effect of EG peptide-linker length on the uptake of micelles targeted with HER2pep(K_0) ($MP_{HER2pep(K0)}$; blue columns) and HER2pep(K_3) ($MP_{HER2pep(K3)}$; red columns) by SK-BR-3 cells. The EG peptide-linker lengths investigated include EG6, EG12, EG18, EG24, EG30, EG36, EG45, and EG72. (D) Effect of oligolysine chain length on cellular uptake by SK-BR-3 cells evaluated with liposomes (blue columns) and micelles (red columns) targeted with HER2pep(K_N)-pep using an EG18 peptide. The K_N content varied in the range $N = 0-4$. (E) Cellular uptake *via* confocal microscopy determined by incubating SK-BR-3 cells with fluorescein-labeled nanoparticles and then counterstaining with LysoTracker Red and Hoechst dyes. Merged images reveal co-localization and internalization of nanoparticles.

cancer system, the model flow system was adopted from previous studies.[47,48] Breast cancer cells (SK-BR-3) were cultured overnight on a tissue culture treated flow channel to promote cell adhesion. Then, a reservoir containing the nanoparticles was connected to the flow channel through a peristaltic pump. For both model systems, the velocity of the flow was regulated by the pump and varied between 5 and 16 cm/s in our experiments to be comparable to the blood flow rates in the circulatory system. The flow channel, reservoirs, and connective tubing were placed inside an incubator to maintain a constant temperature of 37 °C. Fluidic experiments were performed for 1 h, and cellular uptake was analyzed by flow cytometry.

In the fluidic experiments, we examined the effect of EG peptide-linker length and peptide hydrophilicity on the cellular uptake of both VLA-4 and HER2-targeted liposomes and micelles. First, we formulated VLA-4-targeted liposomes and micelles that incorporated VLA4pep(K_3) with variable EG peptide-linker lengths of EG6, EG12, EG18, EG24, EG30, EG36, EG45, and EG72 (Figure 7A and B). Targeted liposomes and micelles were formulated as 93:10:5:2 HSPC:CHOL:PEG2000:VLA4pep(K_3) and 80:10 PEG2000:VLA4pep(K_3), respectively. Although the results for the cellular uptake of micelles under fluidic conditions were similar to those under static conditions with maximum cellular uptake occurring with the use of the EG18 peptide-linker, we observed a distinct shift for optimal peptide-linker length for the liposome system. Under fluidic conditions, an EG18 peptide-linker provided maximum cellular uptake of liposomes, while an EG6 peptide-linker was optimal under static conditions. This can possibly be attributed to the deformation of the liposomes that occurs under fluidic conditions,[49,50] which may necessitate the use of a longer linker to more effectively present the peptide for binding to its target receptor. Additionally, although an EG18 peptide-linker may be less energetically favorable compared to EG6, the extra ~5 nm extension may be

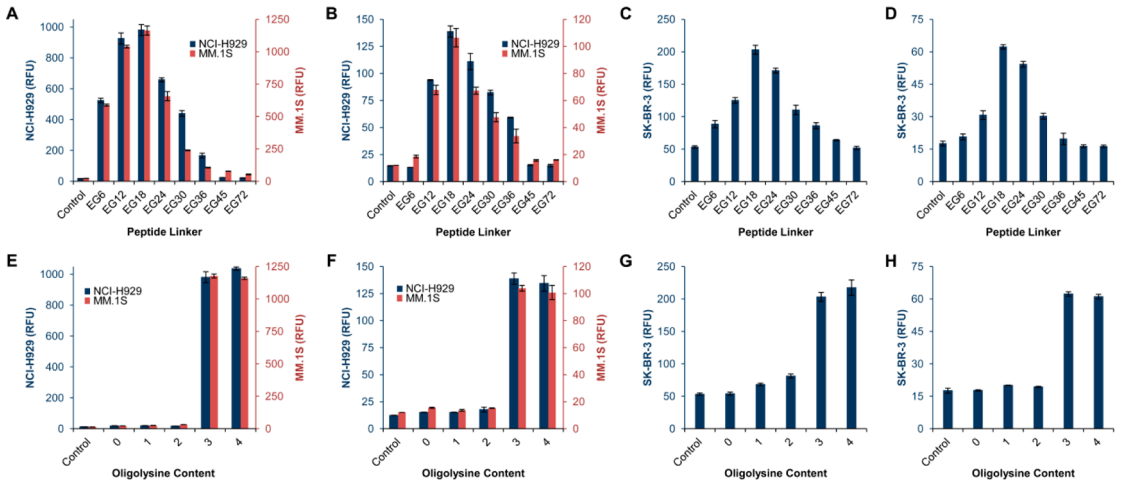

Figure 7. Effect of EG peptide-linker length and oligolysine (K_N) content on the cellular uptake of VLA-4- and HER2-targeted liposomes and micelles under fluidic conditions. The effect of EG peptide-linker length on the cellular uptake of VLA-4-targeted liposomes (A) or micelles (B) using VLA4pep(K_3) was evaluated using NCI-H929 (blue columns) and MM.1S cells (red columns) by flow cytometry. The effect of EG peptide-linker length on the cellular uptake of HER2-targeted liposomes (C) or micelles (D) using HER2pep(K_3) was evaluated using SK-BR-3 cells by flow cytometry. The effect of oligolysine chain length (K_N) was evaluated using liposomes (E) or micelles (F) targeted with VLA4pep(K_N) with EG18 peptide-linker. The effect of oligolysine chain length (K_N) was evaluated using liposomes (G) or micelles (H) targeted with HER2pep(K_N) with EG18 peptide-linker.

imperative for initiating receptor−ligand interactions under fluidic conditions. Importantly, traditional formulations including an EG45 or longer linker in the targeting sequence still resulted in negligible cellular uptake. Next, we evaluated the effect of EG peptide-linker length using HER2-targeted liposomes (93:10:5:2 HSPC:CHOL:PEG2000:HER2pep(K_3)) and micelles (75:15 PEG2000:HER2pep(K_3)) on cellular uptake in fluidic conditions (Figure 7C and D). In the breast cancer system, we observed very similar trends to the experiments performed in static conditions, with an EG18 peptide-linker providing maximum cellular uptake of both liposomes and micelles. Next, we determined the optimal oligolysine chain length under fluidic conditions by formulating VLA-4-targeted liposomes (93:10:5:2 HSPC:CHOL:PEG2000:VLA4pep(K_N)), VLA-4-targeted micelles (80:10 PEG2000:VLA4pep(K_N)), HER2-targeted liposomes (93:10:5:2 HSPC:CHOL:PEG2000:HER2pep(K_N)), and HER2-targeted micelles (75:15 PEG2000:HER2pep-(K_N)) and evaluating cellular uptake (Figure 7E−H). In both cancer models and both nanoparticle types, our results showed minimal cellular uptake with zero to two lysines, but a significant enhancement was observed with the inclusion of three lysines, in agreement with the experiments performed under static conditions. Altogether, these results demonstrated the significance of peptide hydrophilicity and EG peptide-linker length in the efficient cellular uptake of our nanoparticle formulations under physiologically relevant conditions, with an EG18 peptide-linker and three lysine residues providing maximum cellular uptake across all systems analyzed.

CONCLUSION

Nanotechnology has been recognized as a paradigm-changing opportunity by the National Cancer Institute with the potential to make significant breakthroughs in cancer diagnosis and therapy.[51] Ligand-targeted nanoparticles, however, have not consistently delivered successful outcomes.[14−16] In this study, we evaluated how the chemical properties of peptide ligands, specifically their hydrophilicity, the EG peptide-linker length, and peptide valency, affect cellular uptake of peptide-targeted liposomal and micellar nanoparticles. Our results demonstrated, in both the myeloma and breast cancer models, that the cellular uptake of liposomes and micelles can be significantly enhanced by increasing the hydrophilicity of the targeting peptide ligand *via* incorporation of a short oligolysine chain (K_3) adjacent to the targeting peptide. It is noteworthy that, previously, the use of oligoarginine (R8, 8 repeat units of arginine) as a cell-penetrating peptide in liposomes has demonstrated efficiency in promoting cellular uptake through nonreceptor-dependent pathways.[52,53] However, in our design, we selected lysine as the residue of choice due to its much weaker cell-penetrating effects in order to minimize cellular uptake due to nonspecific interactions.[54] Importantly, successful inhibition of cellular uptake during competition experiments using excess soluble peptide demonstrated that the targeted nanoparticles were highly specific and confirmed receptor involvement for the observed cellular uptake.

Our results also demonstrated a strong dependence of cellular uptake on the EG peptide-linker length. In accordance with traditional "stealth" liposome formulations, our design maintained the PEG2000 coating, which has been shown to provide improved stealth and bioavailability to nanoparticles *in vivo*. However, in contrast to the previous groups who have used PEG2000 (~EG45) or longer polymers as ligand

linkers,[19,20] we increased targeting effectiveness by decreasing the length of the EG peptide-linker. Due to the complex structures long PEG polymers adopt on the surface of liposomes[22,23] and micelles,[40] using long linkers such as PEG2000 to present the ligand does not effectively promote binding, as the PEG will sterically hinder the association of the ligand-targeted nanoparticles with their target receptor. Shorter linkers, on the other hand, are more likely to adopt a linear conformation compared to their longer counterparts and will restrict the translational freedom of the peptide, reducing the overall entropic losses upon binding, thereby providing significant thermodynamic advantages in binding to the respective cell surface receptors. Our results validated this hypothesis by demonstrating that EG6 and EG18 linkers provided most effective cellular uptake of VLA-4-targeted liposomes and micelles, respectively. Notably, similar results were also obtained with the HER2-targeted nanoparticles, confirming that our approach is not peptide, receptor, or disease specific. Taken together, these results establish the significance of ligand chemical properties, EG peptide-linker length, and location of ligand–receptor interactions in the cellular uptake of nanoparticles.

In summary, the results presented in this our study demonstrate a universal approach to systematically improve the cellular uptake of peptide-targeted nanoparticles by increasing the hydrophilicity of peptide ligands with oligolysine chains and by using the appropriate EG peptide-linker length. Despite the identification of a wide variety of potential peptides and peptidomimetics as targeting ligands through the use of *in silico* screenings and phage display libraries, not all identified ligands may readily have suitable characteristics to be used in an active-targeting platform.[29−31] For example, chemical properties of the ligand, specifically hydrophobicity, may limit ligand accessibility for binding. Here, we have shown increased cellular uptake of nanoparticles functionalized with both hydrophilic (VLA4pep) and hydrophobic (HER2pep) targeting peptides, both of which have only moderate affinities for their target receptors, demonstrating the widespread application of our method for enhancing active targeting approaches. Importantly, our results established a strategy to achieve favorable results in cellular targeting and uptake, which was otherwise unattainable with traditional targeting strategies. Taken together, this study demonstrates the importance of using the right design elements, such as the appropriate EG peptide-linker length, optimal ligand density, and solubility enhancements, to drive efficient cellular uptake of nanoparticles.

METHODS

Materials. *N*-Fmoc-amino acids, NovaPEG Rink amide resin, Wang resin, 2-(1*H*-benzotriazol-1-yl)-1,1,3,3-tetramethyluronium hexafluorophosphate (HBTU), and bovine serum albumin (BSA) from EMD Millipore (Billerica, MA, USA); Fmoc-$(EG)_n$-OH modification reagents from Quanta Biodesign (Powell, OH, USA); palmitic acid, cholesterol (CHOL), *N,N*-diisopropylethylamine (DIEA), trifluoroacetic acid (TFA), triisopropylsilane (TIS), acetonitrile (ACN), 2-propanol, *N,N*-dimethylformamide (DMF), dichloromethane (DCM), and piperidine from Sigma-Aldrich (St. Louis, MO, USA); fluorescein 5-isothiocyanate (FITC) from Toronto Reseach Chemicals (Toronto, Canada); secondary goat anti-human fluorescein conjugated antibody from Jackson ImmunoResearch (West Grove, PA, USA); 1,2-distearoyl-*sn*-glycero-3-phosphocholine (DSPC), 1,2-dipalmitoyl-*sn*-glycero-3-phosphocholine (DPPC), methoxy PEG2000-DSPE (PEG2000-DPSE), fluorescein PE, and lissamine rhodamine B PE from Avanti Polar Lipids, Inc. (Alabaster, AL, USA) were used.

Humanized mouse mAb Herceptin was provided by Dr. Rudolph Navari (Indiana University School of Medicine).

Synthesis of Peptides and Peptide(K_N)-EG_{linker}-Lipid Conjugates. Ligands were synthesized using Fmoc chemistry on a solid support using Rink amide or Wang resin. Residues were activated with HBTU and DIEA in DMF for 3 min, and coupling efficiency was monitored using the Kaiser test. The Fmoc-protected residues were deprotected with three applications of 20% piperidine in DMF for 3 min each time. The molecules were cleaved from the solid support using a 94/2.5/2.5/1 TFA/H_2O/EDT/TIS mixture twice for 30 min each time. We purified the molecules using RP-HPLC on an Agilent (Santa Clara, CA, USA) 1200 series system with a semipreparative Zorbax C18 column or Zorbax C3 column with either acetonitrile or 2-propanol gradients in the mobile phase. We monitored the column eluent with a diode array detector allowing a spectrum from 200 to 400 nm to be analyzed. The purified product was characterized using a Bruker Autoflex III Smartbeam matrix-assisted laser desorption ionization time-of-flight mass spectrometer (MALDI-TOF-MS, Billerica, MA, USA). Peptide cyclization through disulfide bond formulation was performed in DMF with DIEA under stirring overnight.

Cell Culture. SK-BR-3, NCI-H929, and MM.1S cell lines were obtained from American Type Culture Collection (Rockville, MD, USA). SK-BR-3 cells were cultured in McCoy's 5A (ATCC) media, whereas NCI-H929 and MM.1S cell lines were cultured in RPMI 1640 media (Cellgro, Manassas, VA, USA). All lines were supplemented with 10% fetal bovine serum (FBS), 2 mM L-glutamine (Gibco, Carlsbad, CA, USA), 100 U/mL penicillin, and 100 μg/mL streptomycin (Gibco). NCI-H929 cells were supplemented with an additional 10% FBS and 55 μM 2-mercaptoethanol. MM.1S cells were supplemented with an additional 10% FBS.

Receptor Expression Analysis and Cell-Based Peptide Binding Assays. For VLA-4 expression assays, cells were incubated with anti-CD49d (phycoerythrin) or anti-CD29 (fluorescein) antibodies (BD Biosciences, San Jose, CA, USA) in binding buffer (1.5% BSA in PBS pH 7.4) on ice for 1 h and were washed twice. For HER2 expression assays, cells were incubated with primary antibody in binding buffer on ice for 1 h and washed twice. Fluorescein conjugated secondary antibody was added for 1 h on ice, and samples were washed and analyzed on a Guava easyCyte 8HT flow cytometer (Millipore). Isotype-matched antibodies were used as negative controls. For cell-based peptide binding assays, cells were incubated with increasing concentrations of fluorescein-conjugated peptides for 2 h on ice. Samples were washed twice and analyzed on a Guava easyCyte 8HT flow cytometer.

Nanoparticle Preparation. Liposomes were prepared by dry film hydration. Briefly, a lipid mixture of chloroform stocks was prepared and dried to form a thin film using nitrogen gas, then placed under vacuum overnight to remove residual solvent. The lipid films were hydrated at 65 °C in PBS pH 7.4, gently agitated, and extruded at 65 °C through a 0.1 μm polycarbonate filter. Liposomes all adhered to the formula (95 − *x*): 10:5:*x* HSPC:CHOL:PEG2000-DSPE:peptide(K_N)-EG_{linker}-lipid

conjugate where *x* was varied between 0 and 4 to control the peptide density. Control liposomes were always formulated as 95:10:5 HSPC:CHOL:PEG2000. For micelle formation, nonfunctionalized and functionalized lipids were mixed at desired molar ratios in $CHCl_3$, followed by solvent removal *via* evaporation. The mixture was then resuspended in water and lyophilized to further remove organic solvent. Micelles were formed *via* hydration in PBS and sonicated until clear. The micelles were then centrifuged for 2 min at 15000*g*. Absence of a pellet in conjunction with DLS confirmed micelle formation. If a pellet was observed, sonication followed by centrifugation was performed until no pellet was observed (usually 2−3 cycles). Micelles adhered to the formula (90 − *x*):*x* PEG2000-DSPE: peptide(K_N)-EG_{linker}-lipid conjugate where *x* was varied between 0 and 30 to control the peptide density. Control micelles were always formulated with 100% PEG2000-DSPE. Fluorescein PE was added as a fluorescent agent for cellular uptake quantification.

Characterization of Nanoparticles. Particle size was measured using DLS analysis *via* the 90Plus nanoparticle size analyzer (Brookhaven Instruments Corp., Long Island, NY, USA), using 658 nm light observed at a fixed angle of 90° at 20 °C. Zeta potential was measured using the ZetaPlus zeta potential analyzer (Brookhaven Instruments Corp.).

***In Vitro* Nanoparticle Uptake Assays.** Twenty-four hours prior to each experiment 1×10^5 cells/well were plated in a 24-well dish. Nanoparticles were added at 100 μM phospholipid concentration and incubated for 3 h at 37 °C. Fluorescein PE was added as a fluorescent marker to each nanoparticle formulation. For suspension cells, after incubation, cells were washed three times with PBS and analyzed *via* flow cytometry. For adherent cells, after incubation, cells were washed three times with PBS, trypsinized, and analyzed *via* flow cytometry. Pharmacological inhibition of endocytosis was performed by treating cells with chlorpromazine (30 μM), chloroquine (100 μM), or 5-(*N*-ethyl-*N*-isopropyl)amiloride (EIPA, 50 μM) for 30 min followed by the addition of nanoparticles for 3 h and analysis by flow cytometry.

Confocal Microscopy. Twenty-four hours prior to each experiment 1×10^5 cells/well were plated in a 24-well dish (suspension cells) or onto 12 mm borosilicate glass coverslips (adherent cells). Nanoparticles were labeled with fluorescein PE, added at 100 μM phospholipid concentration, and incubated for 3 h at 37 °C. After incubation, the cells were washed three times with PBS and incubated with 50 nM LysoTracker Red (Molecular Probes, Carlsbad, CA, USA) for 30 min at 37 °C to allow internalization. Cells were washed three times, fixed in PFA, stained with 2 μg/mL Hoechst dye (bisbenzimide H 33342 trihydrochloride, Sigma) for 15 min, washed three times, and mounted on glass slides using Prolong Gold antifade reagent (Molecular Probes). Cells were visualized by a Nikon A1R confocal microscope with a 40× or 100× oil lens (Nikon Instruments, Melville, NY, USA). Image acquisition was performed by Nikon Elements Ar software (Nikon).

Nanoparticle Uptake under Fluidic Conditions. For fluidic assays involving multiple myeloma suspension cells (NCI-H929 and MM.1S), the cells were added to a reservoir connected to a peristaltic pump (Thomas Scientific, Swedesboro, NJ, USA) at a density of 2×10^5 cells/mL in cell growth media and allowed to circulate for 1 min. Nanoparticles were then added to the reservoir at 100 μM phospholipid concentration and allowed to circulate for 1 min. After loading the cells and nanoparticles into the tubing, the reservoir was removed from the system by connecting the reservoir inlet and outlet to create a closed circulating system. The velocity of the flow was regulated by the pump and set to 16 cm/s. Total volume of the circulating system was ~2 mL. The cells and nanoparticles were circulated for 1 h at 37 °C, removed from the circulating system, washed three times with PBS, and analyzed *via* flow cytometry.

For fluidic assays involving adherent breast cancer cells (SK-BR-3), 10^5 cells were seeded on a surface area of 250 mm^2 of a flow channel (μ-Slide ibiTreat from Ibidi, Martinsried, Germany) and allowed to adhere overnight. Nanoparticles were added to a reservoir at 100 μM phospholipid concentration. The reservoir containing the nanoparticles in cell growth media was then connected to the flow channel through a peristaltic pump. The velocity of the flow was regulated by the pump and set to 5 cm/s. At this velocity, approximately 20% of the cells were removed from the surface of the flow channel with more substantial losses at higher velocities. The nanoparticles circulated for 1 h at 37 °C, followed by removal of the flow channel from the system. The cells were then washed three times with PBS to removed residual nanoparticles remaining in the flow chamber, returned to the incubator for 30 min to allow for endocytosis of bound nanoparticles, trypsinized, and then analyzed *via* flow cytometry.

Conflict of Interest: The authors declare no competing financial interest.

Acknowledgment. This work was supported by the Leukemia Research Foundation. We thank the Notre Dame Integrated Imaging Facility for confocal microscopy, the Center for Environmental Science and Technology for the use of DLS and zeta potential, and the Mass Spectrometry and Proteomics Facility for the use of MALDI-TOF-MS.

Supporting Information Available: Mass spectrometry and product yields of peptide(K_N)-EG_{linker}-lipid conjugates, further nanoparticle characterization, confocal microscopy images, and model flow system schematics are available. This material is available free of charge *via* the Internet at http://pubs.acs.org.

REFERENCES AND NOTES

1. Immordino, M. L.; Dosio, F.; Cattel, L. Stealth Liposomes: Review of the Basic Science, Rationale, and Clinical Applications, Existing and Potential. *Int. J. Nanomed.* **2006**, *1*, 297–315.
2. Perche, F.; Torchilin, V. P. Recent Trends in Multifunctional Liposomal Nanocarriers for Enhanced Tumor Targeting. *J. Drug Delivery* **2013**, *2013*, 1–32.
3. Malam, Y.; Loizidou, M.; Seifalian, A. M. Liposomes and Nanoparticles: Nanosized Vehicles for Drug Delivery in Cancer. *Trends Pharmacol. Sci.* **2009**, *30*, 592–599.
4. Allen, T. M.; Cheng, W. W. K.; Hare, J. I.; Laginha, K. M. Pharmacokinetics and Pharmacodynamics of Lipidic Nano-Particles in Cancer. *Anti-Cancer Agents Med. Chem.* **2006**, *6*, 513–523.
5. Allen, T. Liposomal Drug Formulations - Rationale for Development and What We Can Expect for the Future. *Drugs* **1998**, *56*, 747–756.
6. Blanco, E.; Kessinger, C. W.; Sumer, B. D.; Gao, J. Multifunctional Micellar Nanomedicine for Cancer Therapy. *Exp. Biol. Med.* **2009**, *234*, 123–131.
7. Xiao, H.; Stefanick, J. F.; Jia, X.; Jing, X.; Kiziltepe, T.; Zhang, Y.; Bilgicer, B. Micellar Nanoparticle Formation *via* Electrostatic Interactions for Delivering Multinuclear Platinum(II) Drugs. *Chem. Commun.* **2013**, *49*, 4809–4811.
8. Allen, T. Ligand-Targeted Therapeutics in Anticancer Therapy. *Nat. Rev. Cancer* **2002**, *2*, 750–763.
9. Sapra, P.; Tyagi, P.; Allen, T. M. Ligand-Targeted Liposomes for Cancer Treatment. *Curr. Drug Delivery* **2005**, *2*, 369–381.
10. Sofou, S.; Sgouros, G. Antibody-Targeted Liposomes in Cancer Therapy and Imaging. *Expert Opin. Drug Delivery* **2008**, *5*, 189–204.
11. Torchilin, V. Recent Advances with Liposomes as Pharmaceutical Carriers. *Nat. Rev. Drug Discovery* **2005**, *4*, 145–160.
12. Dubey, P.; Mishra, V.; Jain, S.; Mahor, S.; Vyas, S. Liposomes Modified with Cyclic RGD Peptide for Tumor Targeting. *J. Drug Targeting* **2004**, *12*, 257–264.
13. Zhao, X.; Li, H.; Lee, R. J. Targeted Drug Delivery *via* Folate Receptors. *Expert Opin. Drug Delivery* **2008**, *5*, 309–319.
14. Sinha, R.; Kim, G. J.; Nie, S.; Shin, D. M. Nanotechnology in Cancer Therapeutics: Bioconjugated Nanoparticles for Drug Delivery. *Mol. Cancer Ther.* **2006**, *5*, 1909–1917.
15. Ferrari, M. Cancer Nanotechnology: Opportunities and Challenges. *Nat. Rev. Cancer* **2005**, *5*, 161–171.
16. Farokhzad, O. C.; Langer, R. Impact of Nanotechnology on Drug Delivery. *ACS Nano* **2009**, *3*, 16–20.
17. Allen, T. M.; Hansen, C.; Martin, F.; Redemann, C.; Yauyoung, A. Liposomes Containing Synthetic Lipid Derivatives of

Poly(ethylene Glycol) show Prolonged Circulation Half-Lives *in Vivo*. *Biochim. Biophys. Acta* **1991**, *1066*, 29−36.
18. Kirpotin, D.; Park, J.; Hong, K.; Zalipsky, S.; Li, W.; Carter, P.; Benz, C.; Papahadjopoulos, D. Sterically Stabilized Anti-HER2 Immunoliposomes: Design and Targeting to Human Breast Cancer Cells *in Vitro*. *Biochemistry (N. Y.)* **1997**, *36*, 66–75.
19. Gabizon, A.; Horowitz, A.; Goren, D.; Tzemach, D.; Mandelbaum-Shavit, F.; Qazen, M.; Zalipsky, S. Targeting Folate Receptor with Folate Linked to Extremities of Poly-(ethylene glycol)-Grafted Liposomes: *In Vitro* Studies. *Bioconjugate Chem.* **1999**, *10*, 289–298.
20. Yamada, A.; Taniguchi, Y.; Kawano, K.; Honda, T.; Hattori, Y.; Maitani, Y. Design of Folate-Linked Liposomal Doxorubicin to Its Antitumor Effect in Mice. *Clin. Cancer Res.* **2008**, *14*, 8161–8168.
21. Dos Santos, N.; Allen, C.; Doppen, A.; Anantha, M.; Cox, K. A. K.; Gallagher, R. C.; Karlsson, G.; Edwards, K.; Kenner, G.; Samuels, L.; *et al*. Influence of Poly(ethylene glycol) Grafting Density and Polymer Length on Liposomes: Relating Plasma Circulation Lifetimes to Protein Binding. *Biochim. Biophys. Acta-Biomembr.* **2007**, *1768*, 1367–1377.
22. Tirosh, O.; Barenholz, Y.; Katzhendler, J.; Priev, A. Hydration of Polyethylene Glycol-Grafted Liposomes. *Biophys. J.* **1998**, *74*, 1371–1379.
23. Barenholz, Y. Liposome Application: Problems and Prospects. *Curr. Opin. Colloid Interface Sci.* **2001**, *6*, 66–77.
24. Stefanick, J. F.; Ashley, J. D.; Kiziltepe, T.; Bilgicer, B. A Systematic Analysis of Peptide Linker Length and Liposomal Polyethylene Glycol Coating on Cellular Uptake of Peptide-Targeted Liposomes. *ACS Nano* **2013**, *7*, 2935–2947.
25. Forssen, E.; Willis, M. Ligand-Targeted Liposomes. *Adv. Drug Delivery Rev.* **1998**, *29*, 249–271.
26. Schiffelers, R.; Koning, G.; ten Hagen, T.; Fens, M.; Schraa, A.; Janssen, A.; Kok, R.; Molema, G.; Storm, G. Anti-Tumor Efficacy of Tumor Vasculature-Targeted Liposomal Doxorubicin. *J. Controlled Release* **2003**, *91*, 115–122.
27. Reubi, J. Peptide Receptors as Molecular Targets for Cancer Diagnosis and Therapy. *Endocr. Rev.* **2003**, *24*, 389–427.
28. Kiziltepe, T.; Ashley, J. D.; Stefanick, J. F.; Qi, Y. M.; Alves, N. J.; Handlogten, M. W.; Suckow, M. A.; Navari, R. M.; Bilgicer, B. Rationally Engineered Nanoparticles Target Multiple Myeloma Cells, Overcome Cell-Adhesion-Mediated Drug Resistance, and Show Enhanced Efficacy *in Vivo*. *Blood Cancer J.* **2012**, *2*, e64.
29. Torchilin, V. P.; Lukyanov, A. N. Peptide and Protein Drug Delivery to and into Tumors: Challenges and Solutions. *Drug Discovery Today* **2003**, *8*, 259–266.
30. Tan, M. L.; Choong, P. F. M.; Dass, C. R. Recent Developments in Liposomes, Microparticles and Nanoparticles for Protein and Peptide Drug Delivery. *Peptides* **2010**, *31*, 184–193.
31. Pearce, T. R.; Shroff, K.; Kokkoli, E. Peptide Targeted Lipid Nanoparticles for Anticancer Drug Delivery. *Adv. Mater.* **2012**, *24*, 3803–3822.
32. Veronese, F. Peptide and Protein PEGylation: a Review of Problems and Solutions. *Biomaterials* **2001**, *22*, 405–417.
33. Pasut, G.; Guiotto, A.; Veronese, F. Protein, Peptide and Non-Peptide Drug PEGylation for Therapeutic Application. *Expert Opin. Ther. Patents* **2004**, *14*, 859–894.
34. Nobs, L.; Buchegger, F.; Gurny, R.; Allemann, E. Current Methods for Attaching Targeting Ligands to Liposomes and Nanoparticles. *J. Pharm. Sci.* **2004**, *93*, 1980–1992.
35. Lin, K.; Castro, A. Very Late Antigen 4 (VLA4) Antagonists as Anti-Inflammatory Agents. *Curr. Opin. Chem. Biol.* **1998**, *2*, 453–457.
36. Singh, J.; Adams, S.; Carter, M.; Cuervo, H.; Lee, W.; Lobb, R.; Pepinsky, R.; Petter, R.; Scott, D. Rational Design of Potent and Selective VLA-4 Inhibitors and Their Utility in the Treatment of Asthma. *Curr. Top. Med. Chem.* **2004**, *4*, 1497–1507.
37. Jackson, D.; Quan, C.; Artis, D.; Rawson, T.; Blackburn, B.; Struble, M.; Fitzgerald, G.; Chan, K.; Mullins, S.; Burnier, J.; *et al*. Potent Alpha 4 Beta 1 Peptide Antagonists as Potential Anti-Inflammatory Agents. *J. Med. Chem.* **1997**, *40*, 3359–3368.
38. Ashok, B.; Arleth, L.; Hjelm, R.; Rubinstein, I.; Onyuksel, H. *In Vitro* Characterization of PEGylated Phospholipid Micelles for Improved Drug Solubilization: Effects of PEG Chain Length and PC Incorporation. *J. Pharm. Sci.* **2004**, *93*, 2476–2487.
39. Kedar, U.; Phutane, P.; Shidhaye, S.; Kadam, V. Advances in Polymeric Micelles for Drug Delivery and Tumor Targeting. *Nanomed.-Nanotechnol. Biol. Med.* **2010**, *6*, 714–729.
40. Vukovic, L.; Khatib, F. A.; Drake, S. P.; Madriaga, A.; Brandenburg, K. S.; Kral, P.; Onyuksel, H. Structure and Dynamics of Highly PEG-ylated Sterically Stabilized Micelles in Aqueous Media. *J. Am. Chem. Soc.* **2011**, *133*, 13481–13488.
41. Lewis, G. D.; Figari, I.; Fendly, B.; Wong, W. L.; Carter, P.; Gorman, C.; Shepard, H. M. Differential Responses of Human Tumor-Cell Lines to Anti-P185(her2) Monoclonal-Antibodies. *Cancer Immunol. Immunother.* **1993**, *37*, 255–263.
42. Handlogten, M. W.; Stefanick, J. F.; Alves, N. J.; Bilgicer, B. Nonchromatographic Affinity Precipitation Method for the Purification of Bivalently Active Pharmaceutical Antibodies from Biological Fluids. *Anal. Chem.* **2013**, *85*, 5271–5278.
43. Park, B. W.; Zhang, H. T.; Wu, C. J.; Berezov, A.; Zhang, X.; Dua, R.; Wang, Q.; Kao, G.; O'Rourke, D. M.; Greene, M. I.; *et al*. Rationally Designed Anti-HER2/neu Peptide Mimetic Disables p185(HER2/neu) Tyrosine Kinases *in Vitro* and *in Vivo*. *Nat. Biotechnol.* **2000**, *18*, 194–198.
44. Nakajima, H.; Mizuta, N.; Sakaguchi, K.; Fujiwara, I.; Yoshimori, A.; Takahashi, S.; Takasawa, R.; Tanuma, S. Development of HER2-Antagonistic Peptides as Novel Anti-Breast Cancer Drugs by *In Silico* Methods. *Breast Cancer* **2008**, *15*, 65–72.
45. Satyanarayanajois, S.; Villalba, S.; Jianchao, L.; Lin, G. M. Design, Synthesis, and Docking Studies of Peptidomimetics Based on HER2-Herceptin Binding Site with Potential Antiproliferative Activity against Breast Cancer Cell Lines. *Chem. Biol. Drug Des.* **2009**, *74*, 246–257.
46. Berezov, A.; Zhang, H. T.; Greene, M. I.; Murali, R. Disabling ErbB Receptors with Rationally Designed Exocyclic Mimetics of Antibodies: Structure-Function Analysis. *J. Med. Chem.* **2001**, *44*, 2565–2574.
47. Zebli, B.; Susha, A.; Sukhorukov, G.; Rogach, A.; Parak, W. Magnetic Targeting and Cellular Uptake of Polymer Microcapsules Simultaneously Functionalized with Magnetic and Luminescent Nanocrystals. *Langmuir* **2005**, *21*, 4262–4265.
48. del Pino, P.; Munoz-Javier, A.; Vlaskou, D.; Rivera Gil, P.; Plank, C.; Parak, W. J. Gene Silencing Mediated by Magnetic Lipospheres Tagged with Small Interfering RNA. *Nano Lett.* **2010**, *10*, 3914–3921.
49. Beaucourt, J.; Rioual, F.; Seon, T.; Biben, T.; Misbah, C. Steady to Unsteady Dynamics of a Vesicle in a Flow. *Phys. Rev. E.* **2004**, *69*, 011906.
50. Takagi, S.; Yamada, T.; Gong, X.; Matsumoto, Y. The Deformation of a Vesicle in a Linear Shear Flow. *J. Appl. Mech.* **2009**, *76*, 021207.
51. Roco, M. C. The Long View of Nanotechnology Development: The National Nanotechnology Initiative at 10 years. *J. Nanopart. Res.* **2011**, *13*, 427–445.
52. Sharma, G.; Modgil, A.; Sun, C.; Singh, J. Grafting of Cell-Penetrating Peptide to Receptor-Targeted Liposomes Improves their Transfection Efficiency and Transport across Blood-Brain Barrier Model. *J. Pharm. Sci.* **2012**, *101*, 2468–2478.
53. Sharma, G.; Modgil, A.; Layek, B.; Arora, K.; Sun, C.; Law, B.; Singh, J. Cell Penetrating Peptide Tethered Bi-Ligand Liposomes for Delivery to Brain *in Vivo*: Biodistribution and Transfection. *J. Controlled Release* **2013**, *167*, 1–10.
54. Takechi, Y.; Tanaka, H.; Kitayama, H.; Yoshii, H.; Tanaka, M.; Saito, H. Comparative Study on the Interaction of Cell-Penetrating Polycationic Polymers with Lipid Membranes. *Chem. Phys. Lipids* **2012**, *165*, 51–58.